





UNCLASSIFIED

SECURITY CLASSIFICATION OF THIS PAGE(When Data Entered)

20. Abstract (continued)

effect of modulating conditions on working curve slope and linearity is discussed and the limitations of the SLM method are critically evaluated.

UNCLASSIFIED

SECURITY CLASSIFICATION OF THIS PAGE(When Data Entered)

OFFICE OF NAVAL RESEARCH

Contract N14-76-C-0838

Task No. NR 051-622

INDU/DC/GMH/TR-82/45

REDUCTION OF SPECTRAL INTERFERENCES IN  
INDUCTIVELY COUPLED PLASMA-ATOMIC  
EMISSION SPECTROMETRY BY SELECTIVE  
SPECTRAL-LINE MODULATION

by

S. W. Downey and G. M. Hieftje

Prepared for Publication

in

ANALYTICA CHIMICA ACTA

Indiana University  
Department of Chemistry  
Bloomington, Indiana 47405

13 May 1982

Accession For	
NTIS GRA&I	<input checked="" type="checkbox"/>
DTIC TAB	<input type="checkbox"/>
Unannounced	<input type="checkbox"/>
Justification	
By _____	
Distribution/ _____	
Availability Codes	
Dist	Avail and/or Special
A	

Reproduction in whole or in part is permitted for  
any purpose of the United States Government



This document has been approved for public release  
and sale; its distribution is unlimited

Reduction of Spectral Interferences in  
Inductively Coupled Plasma-Atomic  
Emission Spectrometry by Selective  
Spectral-Line Modulation

S. W. Downey and G. M. Hieftje\*

Department of Chemistry  
Indiana University  
Bloomington, Indiana 47405 (U.S.A.)

\*Person to whom correspondance should be addressed

#### SUMMARY

Spectral interferences in inductively coupled plasma (ICP) emission spectrometry can be significantly reduced through the use of selective spectral-line modulation (SLM). In this method, a mirrored, rotating chopper directs the emission from an ICP alternately through and past a flame; selective modulation is achieved when the flame contains absorbing atoms identical to emitting atoms in the ICP. The ability of SLM to minimize broadband, narrow line, and scattered light spectral interferences is demonstrated. Signal-to-background ratios for SLM detection are shown to be higher than those obtained by conventional detection. The effect of modulating conditions on working curve slope and linearity is discussed and the limitations of the SLM method are critically evaluated.

The inductively coupled plasma (ICP) has become a widely used source in atomic emission spectrometry (AES). However, the multi-wavelength advantage offered by AES is also responsible for one of its most problematic drawbacks: spectral interferences. Variable and sometimes subtle, these interferences often complicate elemental quantitation. Unresolvable spectral features from source background, spectral lines from matrix concomitants, and scattered light all contribute to the spectral interference problem.

Most often, high resolution, low stray light spectral dispersing devices are used to reduce spectral interferences. In conjunction with this costly approach, sophisticated software for correction of spectral background and interelement effects have been developed in an attempt to minimize interference from source background and matrix concomitants. Spectral interferences in ICP-AES have also led to the development of spectral-line selection algorithms for multielement analysis. Unfortunately, unambiguous spectral line identification still can be very difficult when complex and/or unknown matrices are being examined. Equally troublesome when measuring an analytical spectral line are wavelength calibration and drift.

Selective modulation of spectral lines of interest offers the high resolution and freedom from spectral interferences afforded by costly spectrometers, yet is simple to employ and provides an automatic wavelength lock to the elemental lines of interest. When desired elemental-line emission alone is modulated and synchronously detected, discrimination against other types of emission is possible.

Previously, selective spectral-line modulation (SLM) has been used in this laboratory to improve continuum-source atomic absorption flame spectrometry

[1,2] and to minimize spectral interferences in flame emission spectrometry [3]. These systems were similar to that used earlier by Alkemade and Milatz [4].

In the present work, an AES-SLM system similar to that of reference 3 was constructed and tested using an ICP as the analytical emission source and with improved optical design. Here, emitted radiation from an ICP is alternately directed through and around a modulating flame by a double-beam optical system. Selective absorption by atoms in the flame creates an element-specific net difference in intensities between the two beam paths, which can then be detected by a lock-in amplifier. All other spectral features not affected (absorbed) by the flame are at a d.c. level and remain undetected.

Because a flame is employed as an atom reservoir, very narrow spectral regions (lines) can be modulated. Consequently, all types of spectral interferences found in the ICP can be reduced greatly by using SLM: narrow-line, broadband, continuum and scattered light. Improved signal-to-background ratios (S/B) are therefore obtained with SLM. Analytical working curves are linear, with their sensitivities (slopes) dependent upon modulating solution concentration.

#### EXPERIMENTAL

A schematic diagram of the SLM detection system used with the ICP is shown in Fig. 1. Details concerning individual components are summarized in Table 1. The system is comprised of three basic units: the emission source (ICP), the double-beam optics, and the detector-demodulator.

A conventional-sized (20 mm o.d.), argon ICP was used with a concentric pneumatic nebulizer-peristaltic pump sample introduction system. The operating conditions of the torch were chosen to conveniently examine many elements and analytical wavelengths without realignment or recalibration of the optical train. Operating parameters were held constant unless otherwise stated.

The emitted radiation from the ICP is transferred to the detector by a series of mirrors. M2 collimates the emitted radiation from the ICP and M3 and M4 focus it onto the entrance slit of the monochromator. The rotating sector mirror, C, and the beam splitter, BS, chop and recombine the beams, producing the double-beam operation necessary for SLM. M1 and M5 are flat, directional mirrors. The placement of the optics is such that a 1:1 image of the ICP is formed at the entrance slit. The vertical slit selects a viewing region in the ICP 15-30 mm above the load coils. The chopper constitutes the limiting aperture of the system, giving a numerical ratio of  $f/10$ . The flame is positioned after the chopper so any flame-based emission will be at a constant level and suppressed by a.c. detection [3]. Air-acetylene and nitrous oxide-acetylene flames were used, depending upon the atomization properties in the flame of the element being studied. The net throughput of both beam paths should be nearly identical to minimize beam imbalances in the SLM system. When such imbalances exist, careful correction is necessary to isolate SLM signals from intrinsic throughput difference effects [3]. Often, this is accomplished with a variable neutral-density filter placed in one beam.

The detector (DET in Fig. 1) consists of a medium-resolution monochromator, used to reduce detector noise, and a standard photomultiplier tube and amplifier. The demodulator (DEMO in Fig. 1) can be any frequency-selective and phase sen-

sitive device. Three such demodulator devices have been tried here: lock-in amplifier, differential-input boxcar integrator and laboratory minicomputer (MINC). Any of these devices can be triggered by a reference signal taken from the chopper. Most wavelength scans reported here were obtained using the lock-in amplifier while most fixed wavelength data were obtained with the MINC minicomputer. The boxcar amplifier was used for initial characterization of the optical train.

The entire optical system is supported by a single, six-foot optical rail bed of the type described by Walters [5].

For comparison purposes, conventional emission data were obtained with the lock-in detection system by blocking entirely the beam path containing the modulating flame. This approach enables the same optical system to be used, providing an appropriate comparison between SLM detection and conventional emission measurement.

All signal-to-noise ratio (S/N) and detection limit calculations were determined in the manner suggested by St. John, et al. [6]. Stock solutions were prepared using reagent-grade metals, salts and acids [7].

## RESULTS AND DISCUSSION

### Reduction of Spectral Interference

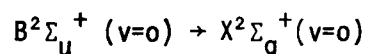
Line Interference. Spectral interference from poorly resolved elemental spectral lines can be extremely troublesome in conventional detection of ICP emission. Routinely, correction factors for spectral line overlap and prudent wavelength selection must be employed even when high-resolution monochromators are used [8]. However, these problems are minimized by SLM detection.

Figure 2 illustrates the ability of the SLM technique to reduce spectral-line interference. Conventional detection of the radiation from an ICP con-

taining a mixture of Cu and Pd is illustrated in spectrum 1. With a monochromator spectral bandpass of 0.1 nm, the Pd (I) 324.3 nm line is just barely resolved from the Cu (I) 324.7 nm line. Other spectral features present are the OH  $A^2\Sigma^+(v=0) \rightarrow X^2\Sigma^+(v=0)$  band, several background spectral lines, and other Cu (I) and Pd (I) lines. Spectrum 2 of Fig. 2 shows the copper-selective SLM-detected spectrum, in which both matrix-based and background spectral lines are suppressed. Graphically evident here is the modulation and detection of the OH band at 306 nm. This behavior is expected, for water and its decomposition products are present in high concentration in the flame, both as a combustion product and from solvent aspiration. Trace 3 is the SLM-detected spectrum obtained when Pd is introduced into the modulating flame. Here Cu and background spectral lines are suppressed. Again it is evident that all absorbers in the flame contribute to the SLM spectrum; the OH band at 306 nm is prominent. Interestingly, the Pd (I) 342.1 nm line visible in Spectrum 1 of Fig. 2 is not present in Spectrum 3. The reason for this absence is that the air-acetylene flame used here cannot sufficiently populate the lower state of the 342.1 nm transition,  $1191\text{ cm}^{-1}$  above the lower state involved in the Pd (I) 324.3 and 340.4 nm lines. Figure 2 also illustrates clearly the spectral simplification and unambiguous spectral line identification offered by SLM detection.

Band Interference. Molecular emission from the ICP consists of band spectra which can interfere with desired elemental spectral lines. Fortunately, the excellent atomization properties of the ICP minimize band emission from sample species. However, band spectra are produced by solvent ( $\text{H}_2\text{O}$ ) vapor and by entrained atmospheric gases and their reaction and fragmentation products. Figure 3 shows the interference of N on three Mo (I) spectral

lines [9]. Spectrum 1 was obtained by conventional detection of the  $N_2^+$



bandhead with three Mo (I) resonance lines superimposed on it. Also present are spectral line features from the ICP background, including, for example, the Ar (I) line at 383.5 nm. Spectrum 2 is the "Mo-selective spectrum", produced by SLM detection with Mo in the modulating flame. Notice the marked suppression of both band and line features from the ICP background.

Another example of the ability of the SLM method to reject unwanted band interference is shown in Fig. 4. In this experiment the monochromator was set on the Bi (I) 306.7 nm resonance line that falls on the R1 bandhead of the OH  $A^2\Sigma^+(v=0) \rightarrow X^2\Sigma^+(v=0)$  transition [9]. As illustrated above (cf. Fig. 2), this OH band is not entirely removed by SLM detection. However, the influence of the OH band can be reduced by employing high concentrations of Bi in the modulating flame. Under these conditions, the absorption spectrum of the modulating flame, and therefore the effective spectral bandpass of the SLM network, is dominated by the Bi line.

Curve 1 in Fig. 4 shows the increase in signal with slit width obtained during conventional detection of the OH background with a blank solution being aspirated into the ICP. Found here is a quadratic dependence of relative intensity upon monochromator slit width, indicative of continuum-like spectral behavior. When Bi is added in relatively high concentration (2.5 mg/mL) to the modulating flame, SLM detection rejects much of the background band emission and provides added specificity for the detection of bismuth (cf. Curve 2, Fig. 4). The slope (1.3) of Curve 2 indicates good discrimination against large amounts of interfering radiation, even though OH in the flame modulates some of the background.

Scattered Light. Elements such as Ca and Mg, when present in high concentration in the ICP, generate strong ionic emission which is known to produce scattered-light-based spectral interferences [10,11]. The SLM approach can significantly reduce this interference as shown in Fig. 5. Curve 1 shows the interference from the Ca (II) 393.3 and 396.8 nm radiation on the Al (I) 396.1 nm spectral line when conventional detection is used. In contrast, Curve 2 shows relative freedom from this interference during SLM detection. The slight upward trend apparent in Curve 2 is caused by the small but finite modulation of the line-broadened Ca (II) radiation that falls exactly at the Al wavelength [10].

Continuum Background Interference. The broad continuum spectral background from the ICP can produce significant spectral interference if background drift occurs, especially if a spectrometer with poor spectral resolution is employed. One cause of drift in the continuum background is variation in rf power into the ICP. In Fig. 6, this situation is simulated by intentional power changes. Curves 1 and 2 of Fig. 6 show the effect of rf power on the conventionally detected signal from Cr (I) emission and background emission, respectively. Curve 2 is very similar to the background behavior at the Cr (I) 357.8 nm line reported by Berman and McLaren [12]. Curve 3 indicates the ability of the SLM method to discriminate against background shifts (in obtaining Curve 3, no special background-correction procedures were employed). Significantly, the SLM-detected Cr signal actually decreases slightly as rf power goes up, in marked contrast to the behavior of Curve 1. This decrease can be explained by the effect of rf power on the spatial emission profile of the Cr line. Edmonds and Horlick [13] report that Cr (I) 425.4 nm emission shifts lower in the ICP as the power is increased. In the present optical

system, emission from lower regions of the ICP would pass through higher spatial regions of the flame where the Cr atom concentration is lower. This change reduces the amount of Cr absorption that takes place, which subsequently decreases the modulated signal. Clearly, it is important to select a constant set of compromise conditions for analysis by the SLM method.

### Multielement Quantitation

To employ SLM for multielement quantitation, several elements can be introduced simultaneously into the modulating flame. Figure 7 illustrates this capability. Trace number 1 of Fig. 7 is the conventionally detected spectrum of emission from the ICP, into which was introduced a solution containing 40  $\mu\text{g/ml}$  each of Cr, Cu and Mg. Spectrum 2 was obtained from the same solution, but using SLM detection, with Cr, Cu and Mg all present in the modulating flame. Importantly, the only features present in spectrum 2 are the atomic resonance lines and the  $A^2\Sigma^+ (v=1) \rightarrow X^2\Sigma^+ (v=0)$  and  $A^2\Sigma^+ (v=0) \rightarrow X^2\Sigma^+ (v=0)$  bands of OH at 281 and 306 nm, respectively. Not surprisingly, the Mg (II) lines at 279.5 and 280.2 nm and the nine Cr (II) lines between 276 and 287 nm are not modulated, because the corresponding ions are not produced in high concentration in the modulating flame.

### Analytical Characteristics

Figure 8 shows the effect of modulating solution concentration on the SLM working curves for Cu. Understandably, higher modulating concentrations produce greater SLM signal amplitudes and correspondingly larger working-curve slopes. Of course, an increase in modulating solution concentration not only increases depth of modulation, but also the width of the modulating

spectral interval. Moreover, high modulating solution concentrations would limit the number of elements which could be simultaneously modulated, because of possible problems with sample introduction into the flame. Finally, many elements, unlike copper, emit strongly and would generate substantial detector shot noise if present in the modulating flame in high concentration. Consequently, the lower modulating solution concentrations employed in Fig. 8 (Curve 2 or 3) would be preferred in most analytical situations where extremely high detection sensitivity is not required.

A substantial advantage of SLM detection over conventional detection is the improvement in signal-to-background ratio (S/B) revealed in Fig. 9. In Fig. 9, Curve 2, the background signal for SLM was taken when a blank solution was sprayed into the ICP and when a copper solution was introduced into the flame. Clearly, a much smaller portion of the spectral background is modulated, compared to the amount of background detected conventionally (Curve 1). As expected, the conventionally detected background increases as the square of the slit width, while the signal increases linearly with slit width. The net effect is the lowering of S/B (Curve 1). However, the decrease in S/B with slit width is small for the SLM method (Curve 2) because of the narrow absorbing-line profile in the flame.

Figure 10 explores this behavior in more detail. Curves 1 and 2 show the quadratic and linear dependence of intensity on slit width of the background and analyte signal, respectively. Unlike conventional detection, the background intensity detected in the SLM method, shown in Curve 4, has a slope less than 2 and, in fact, approaches unity. This behavior illustrates the line-like character of SLM detection. Because of this capability, large slit widths could be employed with SLM instruments in light-limited situations,

although S/N would not be expected to improve. As expected, the slope of Curve 3, the copper signal with SLM detection, is nearly unity. Curves 1 and 3 compare favorably to the Bi data of Fig. 4.

Upon comparison, the slopes of Curves 2 and 3 of Fig. 10 are the same to within experimental error. This indicates that under these conditions, the absorption spectral line width in the flame is wider than the emission spectral line width of the ICP. Also, the absolute magnitude of Curve 3 is less than that of Curve 2 indicating the incomplete absorption intrinsic in any absorption experiment. As a result, the sensitivity of the SLM method will be slightly lower than the sensitivity of conventional detection.

Table 2 compares several characteristics of SLM and conventional detection of a number of elements at the part-per-million level. The conventional emission data were obtained on the same dual-beam system used for SLM but with the flame-containing path blocked. Overall, signal-to-background ratios are ten times higher with SLM, although signal-to-noise ratios (S/N) are slightly lower, except in two cases. As a result, detection limits were somewhat poorer with SLM. A comparison of these detection limits with those in the literature [15] suggests that the dual-beam optical system used in this study is not particularly efficient and seems rather noisy. Of course, a portion of this increased noise originates in the modulating flame.

It is also evident in Table 2 that no correction is necessary for most interelement effects with SLM. Sample-matrix-based interfering spectral lines have exceedingly small effects. Calibration for spectral interferences [11,16] will therefore seldom be necessary with SLM.

Attempts to modulate ion lines using a nitrous oxide-acetylene flame were only marginally successful and would probably not be routinely useful.

For example, the U (II) line at 409.0 nm was not detectable even at modulating solution concentrations of 10 mg/ml. However, the Ca (II) 393.3 nm line exhibited slight modulation, consistent with the work of Koirtyohann and Lichte [17]. In general, resonance atomic lines are best suited to detection by SLM with a modulating flame.

Unfortunately, the use of high-temperature modulating ion reservoirs is unattractive. Such sources normally have small absorbing path lengths, broadened lines and greater background emission [3,18]. For these reasons, the SLM method seems at present unlikely to benefit from the frequently heralded "ion-line advantage" of the ICP.

#### CONCLUSION

From this work, it is apparent that the greatest advantages offered by the SLM method are element specificity and wavelength selectivity. For this reason, SLM seems best suited for nonroutine examination of unusually complex ICP emission spectra and routine situations where high resolution instrumentation is impractical.

In the present system, the SLM method is not suited for work where sub-trace detection limits are required or for the quantitation of elements that do not have atomic lines terminating in low-lying states in the ICP.

This work was supported in part by the Office of Naval Research and by the National Science Foundation through grant CHE 79-18073.

## REFERENCES

1. R. L. Cochran and G. M. Hieftje, *Anal. Chem.*, 49 (1977) 98.
2. R. L. Cochran and G. M. Hieftje, *Anal. Chem.*, 50 (1978) 791.
3. S. W. Downey, J. G. Shabushnig and G. M. Hieftje, *Anal. Chim. Acta*, 121 (1980) 165.
4. C. T. J. Alkemade and J. M. W. Milatz, *Appl. Sci. Res.*, 48 (1955) 289.
5. J. P. Walters, "A Synergic Approach to Graduate Research in Spectroscopy and Spectrochemical Analysis", Ch. 3 in *Contemporary Topics in Analytical and Clinical Chemistry*, Vol. 3, D. M. Hercules, G. M. Hieftje, L. R. Snyder and M. A. Evenson, Eds., Plenum, 1978.
6. P. A. St. John, W. J. McCarthy and J. D. Winefordner, *Anal. Chem.*, 39 (1969) 1495.
7. J. A. Dean and T. C. Rains, *Flame Emission and Atomic Absorption Spectrometry*, Vol. II, M. Dekker, New York, 1969, Ch. 13.
8. J. W. McLaren, S. S. Berman, U. J. Boyko and D. S. Russell, *Anal. Chem.*, 52 (1981) 1802.
9. R. W. B. Pearse and A. G. Gaydon, *The Identification of Molecular Spectra*, John Wiley & Sons, New York, 1941.
10. G. F. Larson, V. A. Fassel, R. K. Winge and R. N. Kniseley, *Appl. Spectrosc.*, 30 (1976) 384.
11. C. E. Taylor and T. L. Floyd, *Appl. Spectrosc.*, 34 (1980) 472.
12. S. S. Berman and J. W. McLaren, *Appl. Spectrosc.*, 32 (1978) 372.
13. T. E. Edmonds and G. Horlick, *Appl. Spectrosc.*, 31 (1977) 536.
14. N. Omenetto, S. Nikdel, J. D. Bradshaw, M. S. Epstein, R. D. Reeves and J. D. Winefordner, *Anal. Chem.*, 51 (1979) 1521.

15. P. W. J. M. Boumans, *Spectrochim. Acta*, 36B (1981) 169.
16. G. W. Johnson, H. E. Taylor and R. K. Skogerboe, *Appl. Spectrosc.*, 33 (1979) 451.
17. S. R. Koirtyohann and F. E. Lichte, *Can. J. Spectrosc.*, 23 (1978) 98.
18. G. Horlick, personal communication, 1981.

Table 1

System Components and Operating Conditions for ICP-SLM

Inductively Coupled Plasma

Model HFP-2500F, 2.5 kW, 27.12 MHz with model AMN-PS-1 automatic impedance matcher (Plasma-Therm, Inc., Kresson, NJ)

Input Power 1kW

Gas Flow Rates (Ar)    Coolant:    16 l/min  
                                  Plasma:    0.5 l/min  
                                  Nebulizer: 0.9 l/min

Gas Handling:            Bulk liquid Ar, (Minewald Co., Indianapolis, IN) controlled by needle valves, monitored by calibrated rotameters (Matheson Co., Joliet, IL)

Sample Solution Uptake:            1.0 ml/min delivered by peristaltic pump (Minipuls 2, Gilson Medical Electronics, Inc., Middleton, WI)

Nebulizer:              Concentric glass type

Torch:                    20 mm O.D.

Flame:                    Supported on slot burner equipped with impinging bead nebulizer (Instrumentation Laboratory, Inc., Wilmington, MA)  
                                  air/acetylene; 10 cm slot  
                                  N<sub>2</sub>O/acetylene; 5 cm slot

Flame Gas Flow Rates:            air; 15 l/min    C<sub>2</sub>H<sub>2</sub>; 3 l/min  
                                  N<sub>2</sub>O; 3 l/min    C<sub>2</sub>H<sub>2</sub>; 2 l/min

Flame Gas Handling:    Purified flame gases (Matheson Co., Joliet, IL) controlled by needle valves (Series M, Nupro Co., Cleveland, OH) monitored by calibrated rotameters (No. VFB, Dwyer Instruments, Inc., Michigan City, IN)

Flame Solution Uptake Rate:    4 ml/min

Optics

Monochromator:        EU 700 GCA/McPherson Instruments (Acton, MA), 0.35 m Czerny-Turner mount, slit width 50 μm, 1 Å spectral bandpass.

Chopper:                Butterfly configuration, Model RC45 (Valtec, Costa Mesa, CA) 4.5 in diameter front-surface aluminum with MgF<sub>2</sub> overcoat. Rotated at 38 Hz by synchronous motor.

Plane Mirrors: M1, M5; 2 in. diameter front-surface aluminum with MgF<sub>2</sub> overcoat (Oriel Corp., Stamford, CN).

Concave Mirrors: M2, M3, M4; 4 in. diameter front-surface aluminum with MgF<sub>2</sub> overcoat, focal length; 50 cm. (3B Optical, Gibsonia, PA).

Beam Combiner: 2 in. x 2 in. u.v. beamsplitter, model SU 51X (Optics for Research, Caldwell, NJ) 33% T, 33% R for 200-500 nm.

Optical Mounts: Model 625A-2, 625A-4 mirror mounts (Newport Research Corp., Fountain Valley, CA).

#### Detection

Photomultiplier: Hamamatsu R106, operated at 800-1000 V, supplied by Model 244 high-voltage power supply (Keithley Instruments, Cleveland, OH).

Amplifier: High-speed current amplifier, model 427 (Keithley Instruments, Cleveland, OH).

Reference Detector: TIL 149 i.r. source and sensor assembly triggered by chopper.

#### Demodulation

Lock-in Amplifier: Model 220 lock-in amplifier (Princeton Applied Research Corp., Princeton, NJ).

Minicomputer: Digital Equipment Corp. MINC-11/03 laboratory mini-computer (Maynard, MA)

Boxcar Amplifier: Model 162 Boxcar averager with model 164 input gates (Princeton Applied Research Corp., Princeton, NJ).

Recorder: Model SR-204 strip chart type, operated at 10 V full scale (Heath Co., Benton Harbor, MI).

Table 2

## Analytical Characteristics of ICP-SLM

Element	Ag (I)	Cr (I)	Cu (I)	Cu (I)	In (I)	Mg (I)
Wavelength (nm)	328.1	425.4	324.7	327.4	325.6	285.2
Signal/Background for 1 $\mu\text{g/ml}$						
Emission	0.07	0.03	1.0	0.05	0.016	0.27
SLM <sup>a</sup>	2.0	0.13	4.4	0.43	0.30	1.2
Signal/Noise for 1 $\mu\text{g/ml}$						
Emission	6.0	6.0	17	9.0	2.0	30
SLM <sup>a</sup>	2.0	2.0	35	3.0	3.7	25
Detection Limit ( $\mu\text{g/ml}$ )						
Emission	0.1	0.35	0.08	0.2	1.0	0.07
SLM <sup>a</sup>	1.0	1.0	0.04	0.7	0.6	0.12
Literature <sup>b</sup>	0.0047	0.0093	0.0036	0.0065	0.08	0.0011
INTERFERENCES						
Interfering Species	Zr (II)	Continuum	OH	Zr (II)	Cd (I)	OH
Wavelength (nm)	327.9	Broad	Broad	327.3	326.1	Broad
Type	Line	Background	Band	Line	Line	Band
Amount of interfering species equivalent to 1 $\mu\text{g/ml}$ analyte	150 $\mu\text{g/ml}$	c	c	200 $\mu\text{g/ml}$	470 $\mu\text{g/ml}$	c
Interfering species Contribution to SLM signal <sup>a</sup>	e	d	d	e	e	d

<sup>a</sup>10,000  $\mu\text{g/ml}$  analyte sprayed into air/acetylene modulating flame

<sup>b</sup>P.W.J.M. Boumans, Spectrochim. Acta 36B, 169 (1981)

<sup>c</sup>Decreases S/B in conventional detection

<sup>d</sup>Reduced by SLM

<sup>e</sup>None detected

## FIGURE LEGENDS

- Figure 1. Schematic diagram of double-beam SLM system. M1, M5, flat mirrors; M2, M3, M4, spherically concave mirrors, C, rotating sector mirror; BS, beamsplitter used to combine beams; DET, monochromator and detector; DEMO, demodulating electronics and data storage. See Table 1 for details of components. The dimensions of the entire optical array are approximately 50 x 100 cm.
- Figure 2. SLM reduction of copper and palladium line interferences on each other. (1) Spectrum obtained using conventional detection of emission from 40  $\mu\text{g/ml}$  Cu and 80  $\mu\text{g/ml}$  Pd in ICP; (2) Cu-selective SLM spectral scan using 1 mg/ml Cu in modulating flame; (3) Pd-selective SLM spectral scan using 1 mg/ml Pd in modulating flame.
- Figure 3. SLM reduction of  $\text{N}_2^+$  band interference on three molybdenum spectral lines (1) Conventional emission spectrum of ICP containing 40  $\mu\text{g/ml}$  Mo; (2) Spectrum obtained using SLM detection with 10 mg/ml Mo in modulating flame.
- Figure 4. SLM reduction of OH band interference on bismuth. (1) Effect of slit width on conventionally detected signal from blank solution in ICP; increase caused by OH band; (2) SLM detection of 250  $\mu\text{g/ml}$  Bi in ICP using 2.5 mg/ml Bi in modulating flame. See text for details.

Figure 5. Reduction by SLM of Ca (II) scattered light interference on aluminum. A solution of 100  $\mu\text{g/ml}$  Al was nebulized into the ICP. Spectral slit width, 0.6 nm. (1) Conventional detection; (2) SLM detection using 10 mg/ml Al in a nitrous oxide-acetylene modulating flame.

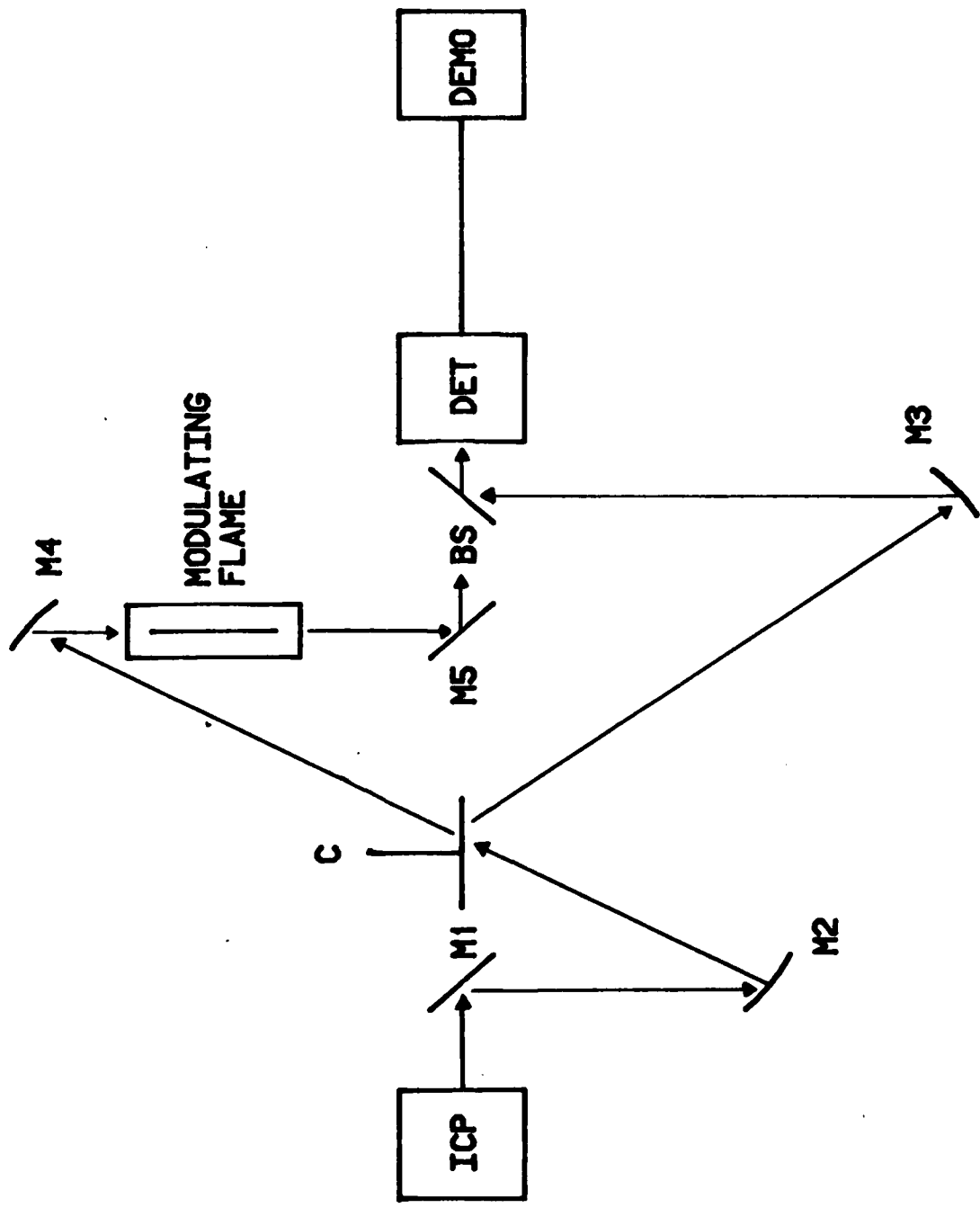
Figure 6. Reduction of continuum background interference by the SLM method. (1) Effect of rf power on the background-corrected signal from 100  $\mu\text{g/ml}$  Cr (conventional detection); (2) Effect of applied rf power on ICP background (conventional detection); (3) Effect of rf power on the signal from 100  $\mu\text{g/ml}$  Cr in ICP (SLM detection); 1 mg/ml Cr nebulized into modulating flame. See text for details.

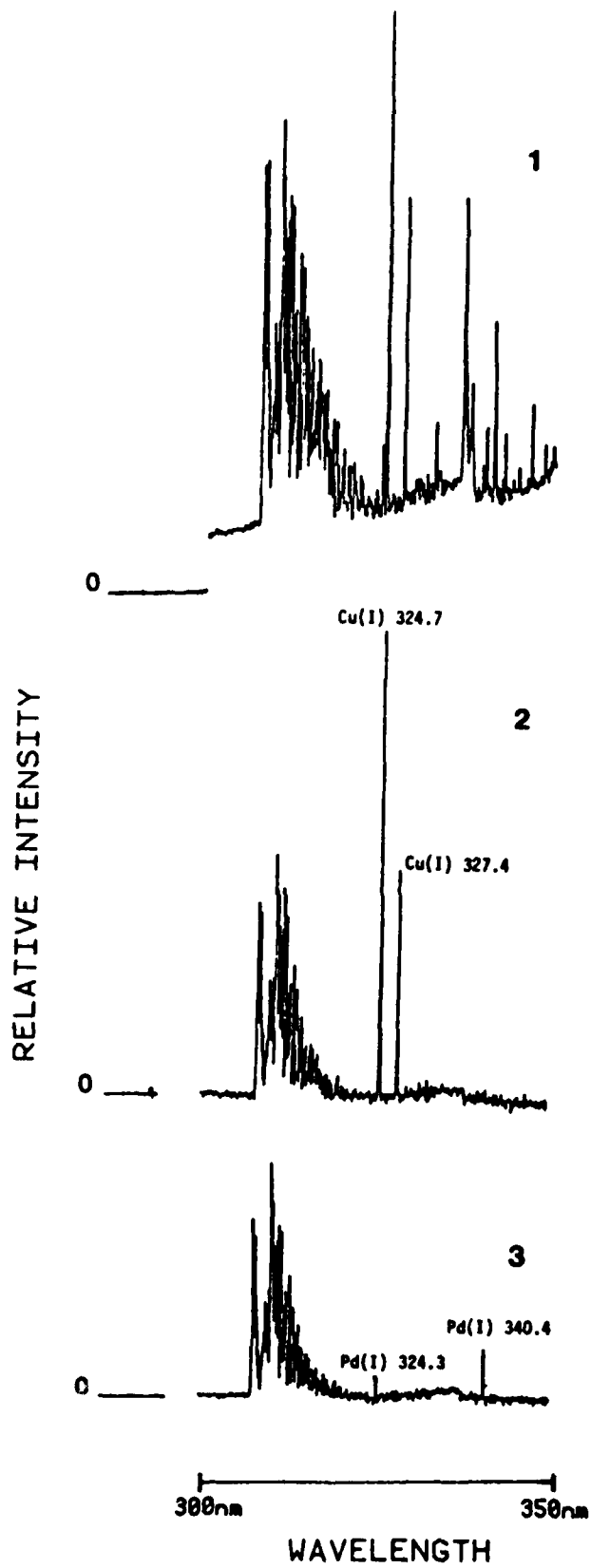
Figure 7. Reduction of ICP background in multielement SLM analysis. (1) Conventionally detected spectrum of 40  $\mu\text{g/ml}$  each of Cr, Cu and Mg in ICP; (2) SLM-detected spectrum of same solution; 1 mg/ml each Cr, Cu and Mg employed in modulating flame. See text for details.

Figure 8. Effect of modulating solution concentration on the SLM-detected working curves for copper. Concentration of Cu in modulating flame (mg/ml): (1) 10; (2) 1; (3) 0.1.

Figure 9. Influence of monochromator slit width on S/B for SLM and conventional detection. (1) Conventional detection of 10  $\mu\text{g}/\text{ml}$  Cu in ICP. (2) SLM detection using 10  $\text{mg}/\text{ml}$  Cu in modulating flame.

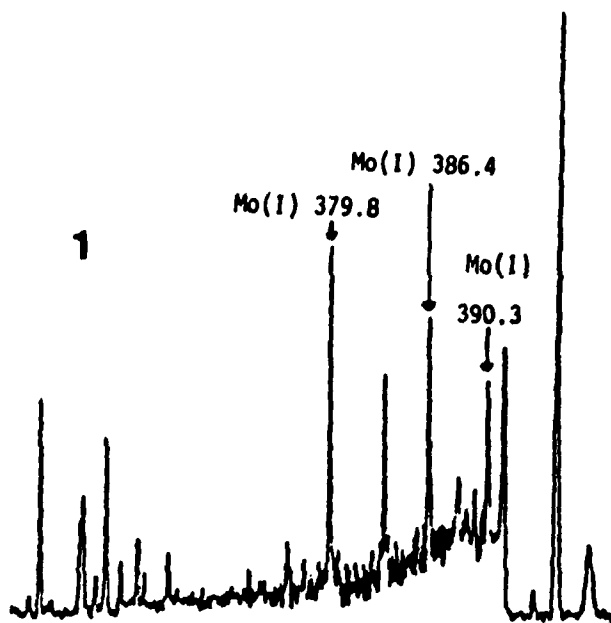
Figure 10. Conventional detection of: (1) Blank (background) in ICP; (2) 10  $\mu\text{g}/\text{ml}$  Cu in ICP. SLM detection using 10  $\text{mg}/\text{ml}$  Cu in modulating flame of: (3) 10  $\mu\text{g}/\text{ml}$  Cu in ICP; (4) Blank background in ICP.



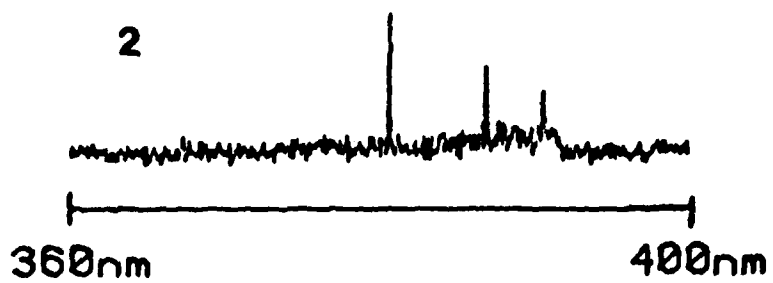


RELATIVE INTENSITY

0

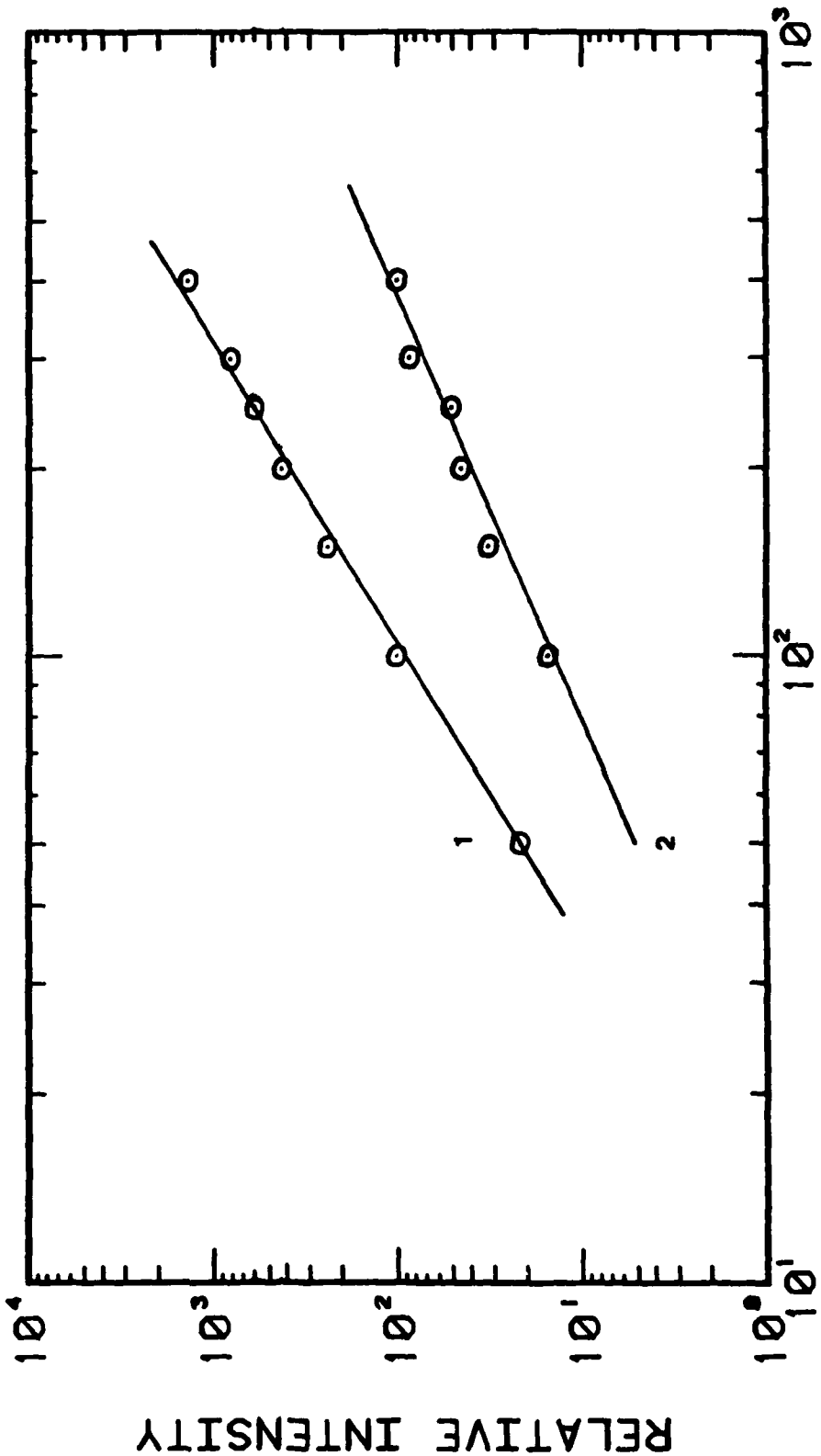


0

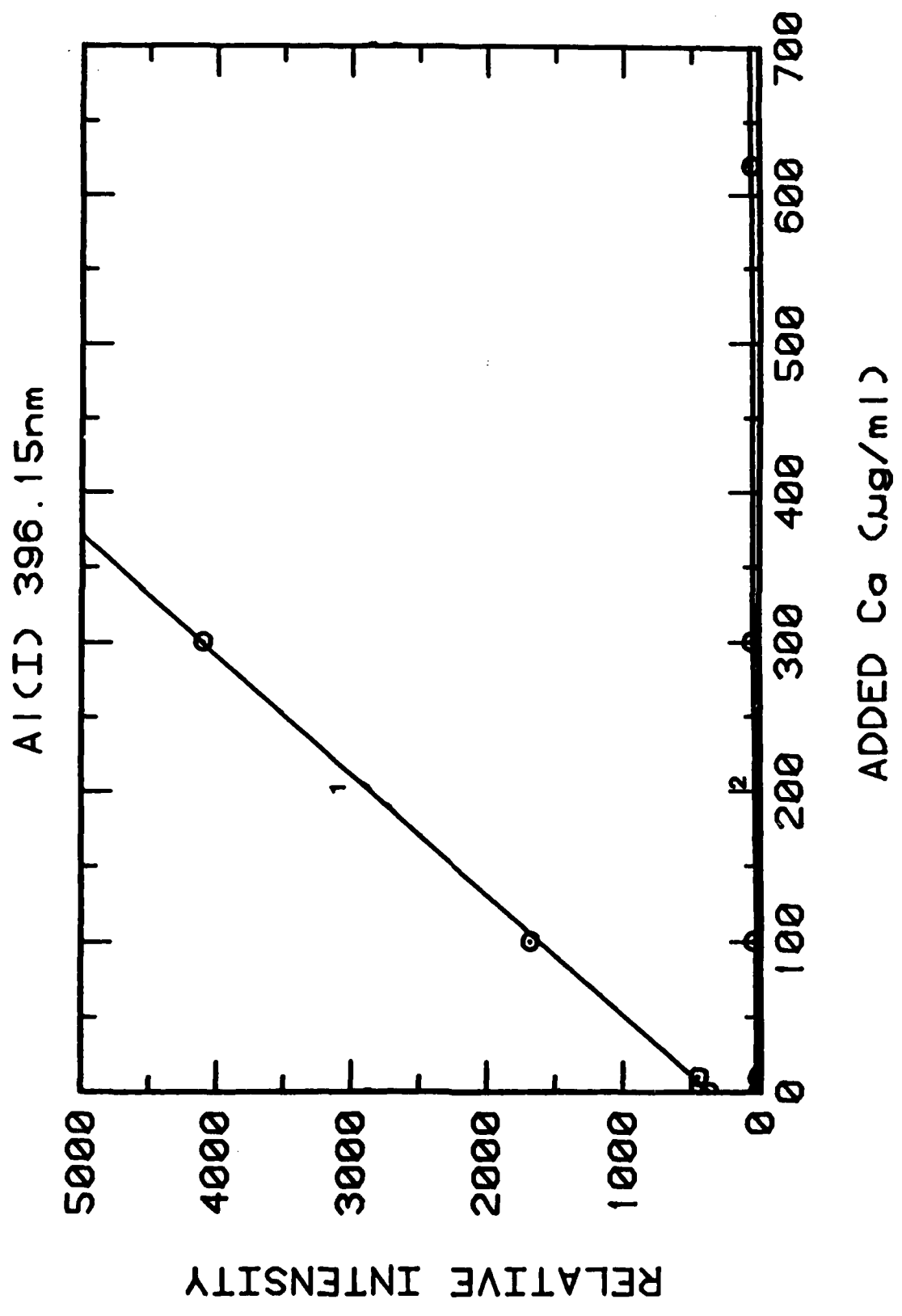


WAVELENGTH

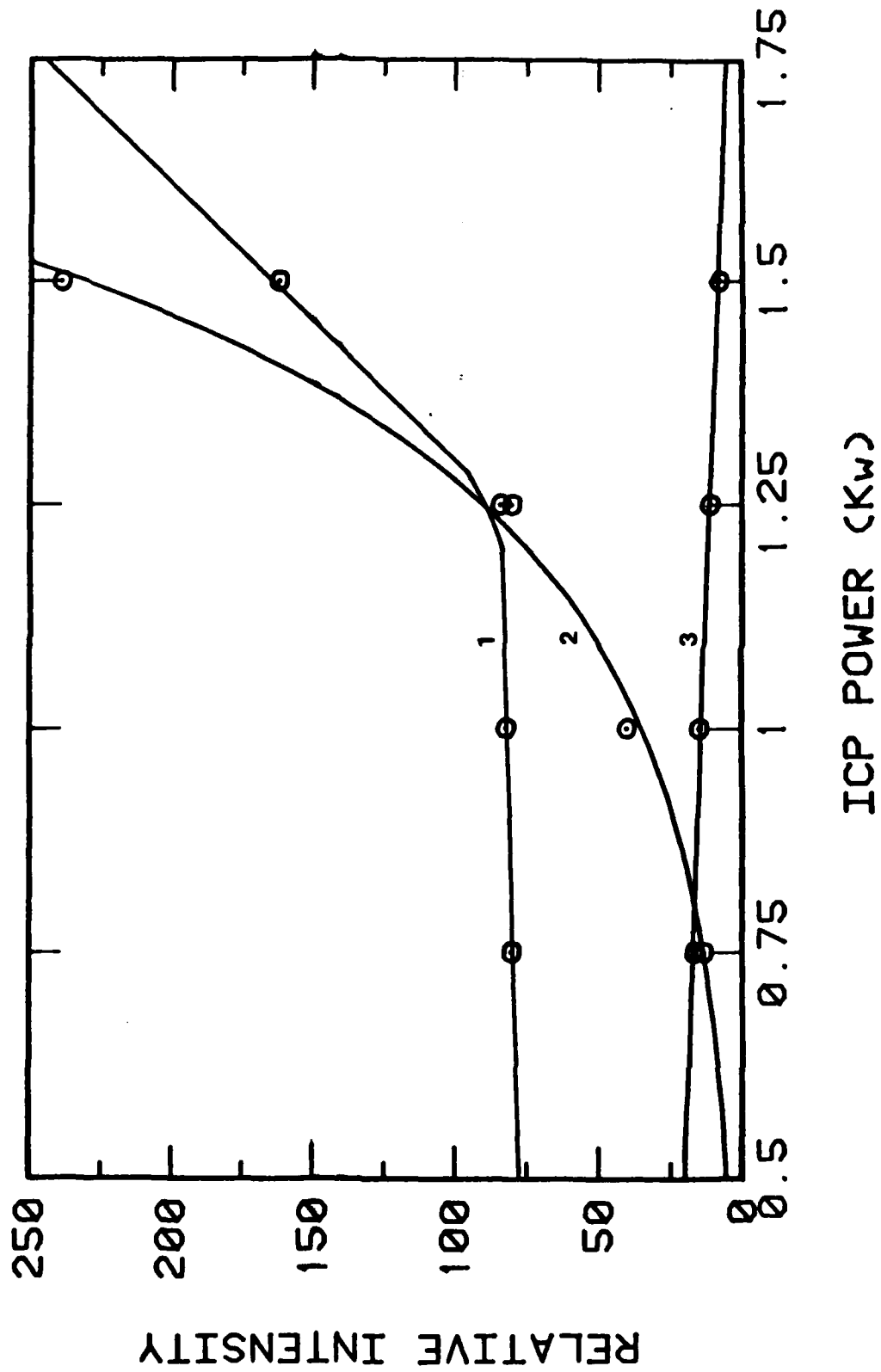
Bi (I) 306.7nm

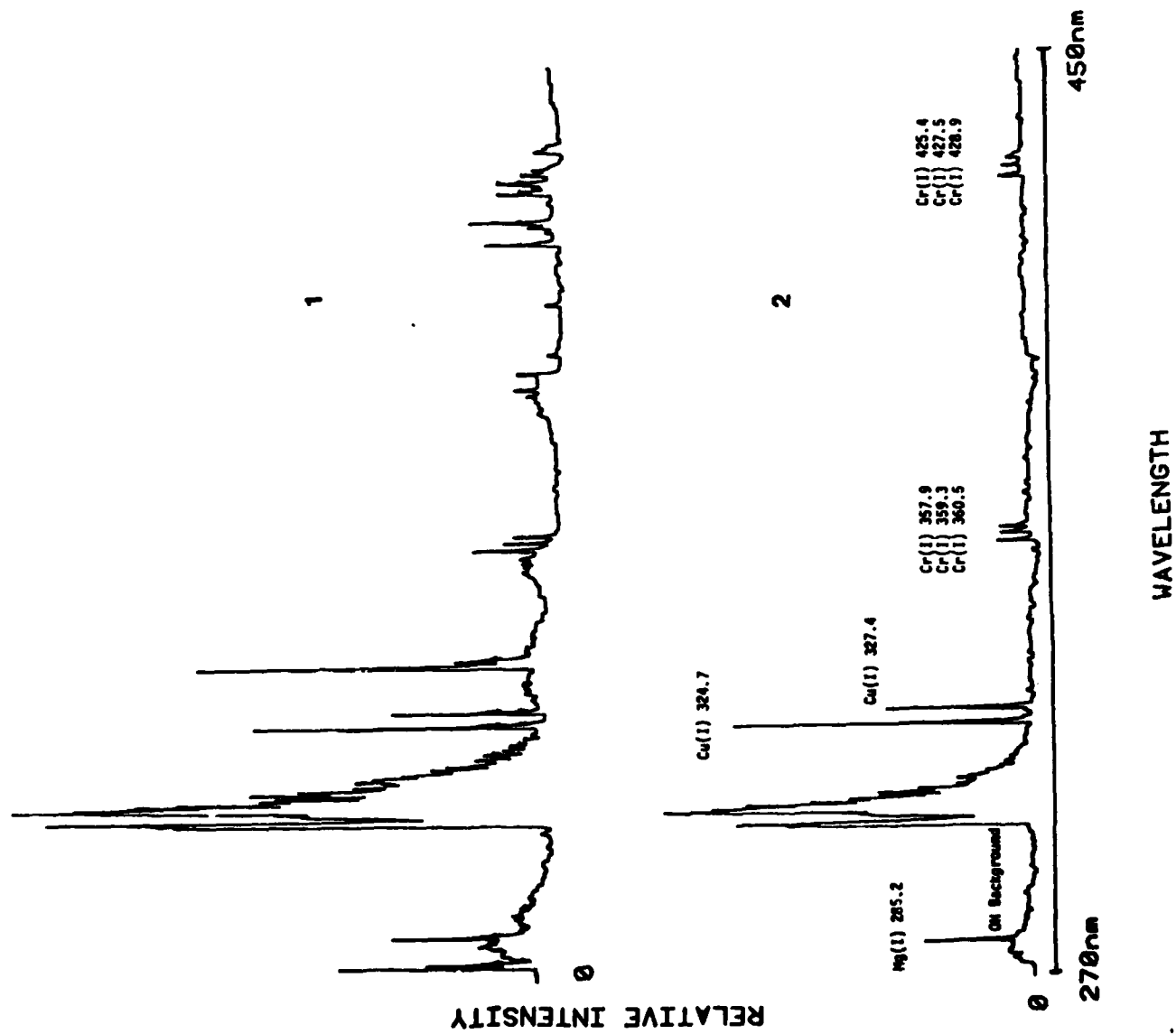


SLIT WIDTH (μm)

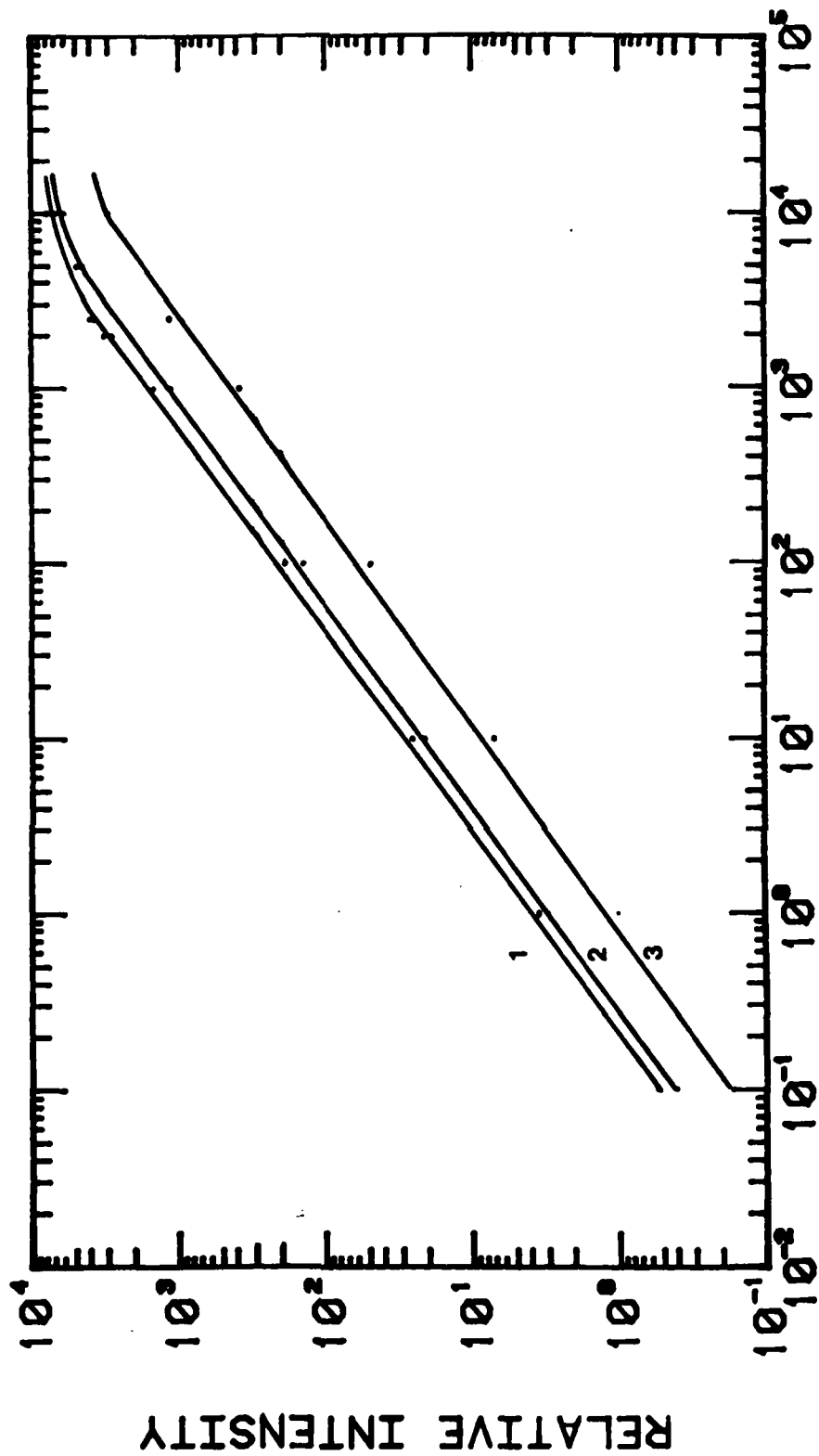


Cr (I) 425.4nm



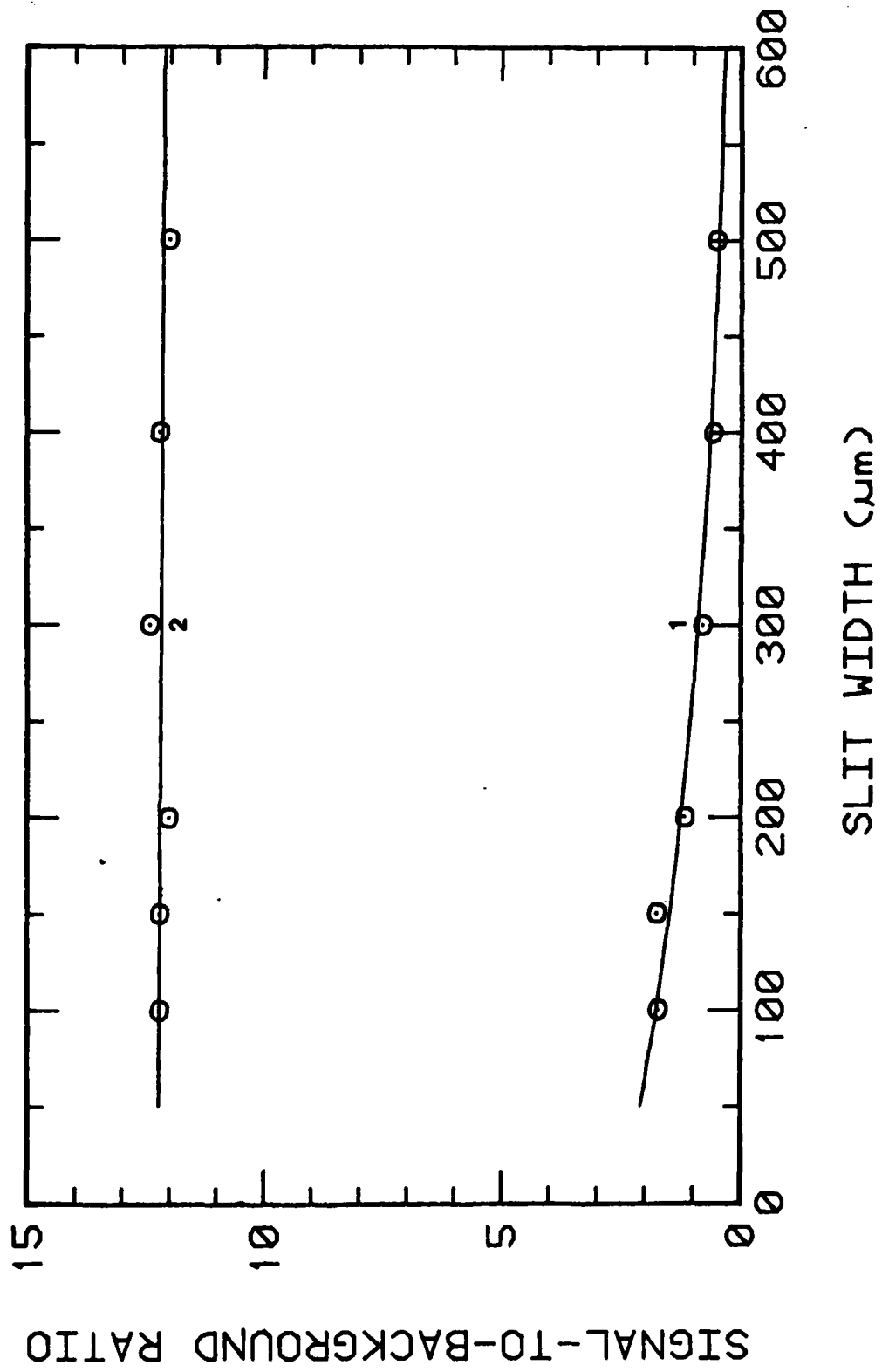


Cu (I) 324.7nm

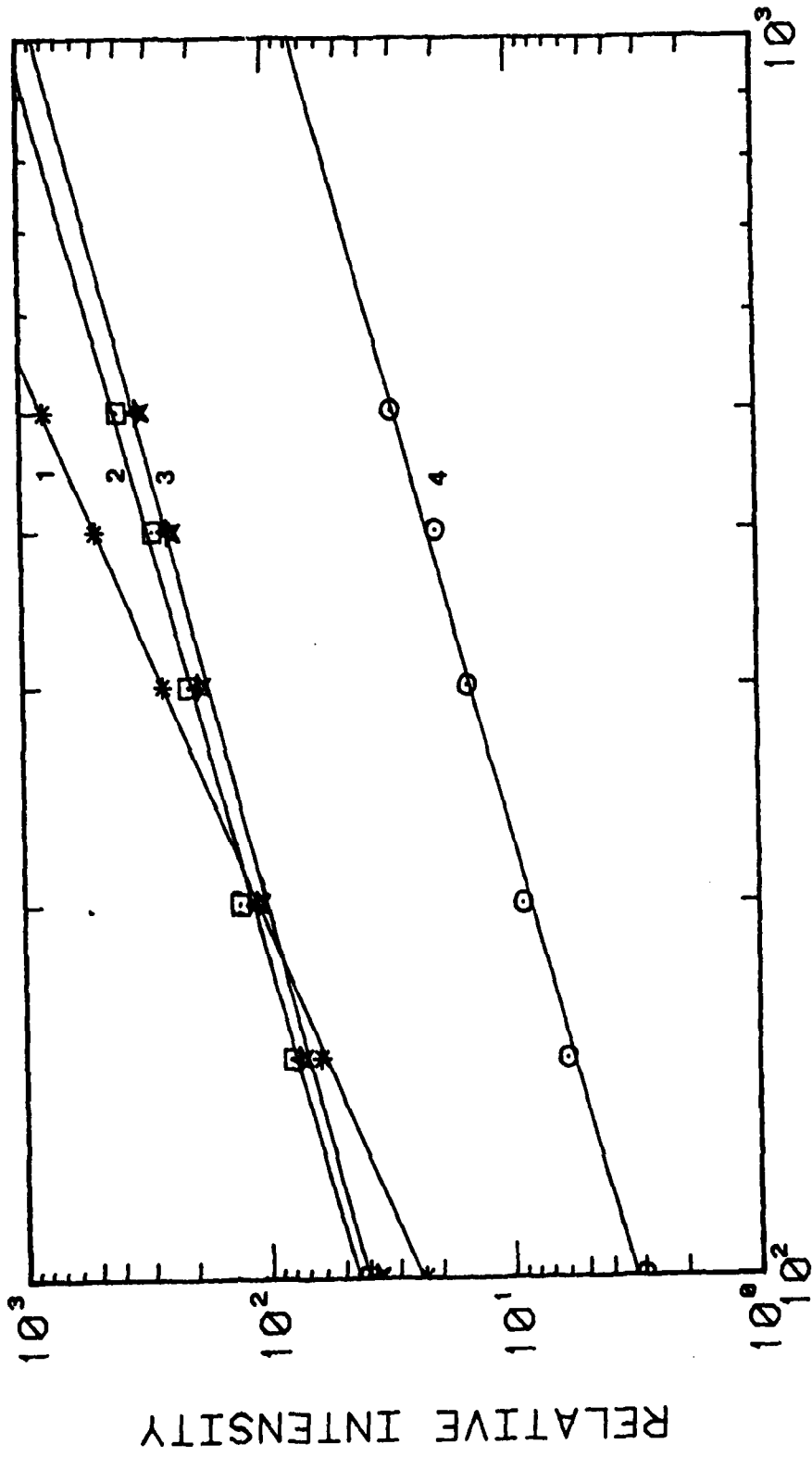


Cu concentration in ICP (µg/ml)

Cu (I) 324.7nm



Cu (I) 324.7nm



TECHNICAL REPORT DISTRIBUTION LIST, 051C

	<u>No. Copies</u>		<u>No. Copies</u>
Dr. M. B. Denton Department of Chemistry University of Arizona Tucson, Arizona 85721	1	Dr. John Duffin United States Naval Postgraduate School Monterey, California 93940	1
Dr. R. A. Osteryoung Department of Chemistry State University of New York at Buffalo Buffalo, New York 14214	1	<del>Dr. G. M. Hieftje Department of Chemistry Indiana University Bloomington, Indiana 47401</del>	1
Dr. B. R. Kowalski Department of Chemistry University of Washington Seattle, Washington 98105	1	Dr. Victor L. Rehn Naval Weapons Center Code 3813 China Lake, California 93555	1
Dr. S. P. Perone Department of Chemistry Purdue University Lafayette, Indiana 47907	1	Dr. Christie G. Enke Michigan State University Department of Chemistry East Lansing, Michigan 48824	1
Dr. D. L. Venezky Naval Research Laboratory Code 6130 Washington, D.C. 20375	1	Dr. Kent Eisentraut, MBT Air Force Materials Laboratory Wright-Patterson AFB, Ohio 45433	1
Dr. H. Freiser Department of Chemistry University of Arizona Tucson, Arizona 85721		Walter G. Cox, Code 3632 Naval Underwater Systems Center Building 148 Newport, Rhode Island 02840	1
Dr. Fred Saalfeld Naval Research Laboratory Code 6110 Washington, D.C. 20375	1	Professor Isiah M. Warner Texas A&M University Department of Chemistry College Station, Texas 77840	1
Dr. H. Chernoff Department of Mathematics Massachusetts Institute of Technology Cambridge, Massachusetts 02139	1	Professor George R. Morrison Cornell University Department of Chemistry Ithaca, New York 14853	1
Dr. K. Wilson Department of Chemistry University of California, San Diego La Jolla, California	1	Professor J. Janata Department of Bioengineering University of Utah Salt Lake City, Utah 84112	1
Dr. A. Zirino Naval Undersea Center San Diego, California 92132	1	Dr. Carl Heller Naval Weapons Center China Lake, California 93555	1

TECHNICAL REPORT DISTRIBUTION LIST, GEN

	<u>No. Copies</u>		<u>No. Copies</u>
Office of Naval Research Attn: Code 472 800 North Quincy Street Arlington, Virginia 22217	2	U.S. Army Research Office Attn: CRD-AA-IP P.O. Box 1211 Research Triangle Park, N.C. 27709	1
ONR Western Regional Office Attn: Dr. R. J. Marcus 1030 East Green Street Pasadena, California 91106	1	Naval Ocean Systems Center Attn: Mr. Joe McCartney San Diego, California 92152	1
ONR Eastern Regional Office Attn: Dr. L. E. Peebles Building 114, Section D 666 Summer Street Boston, Massachusetts 02210	1	Naval Weapons Center Attn: Dr. A. B. Amster, Chemistry Division China Lake, California 93555	1
Director, Naval Research Laboratory Attn: Code 6100 Washington, D.C. 20390	1	Naval Civil Engineering Laboratory Attn: Dr. R. W. Drisko Port Hueneme, California 93401	1
The Assistant Secretary of the Navy (RE&S) Department of the Navy Room 4E736, Pentagon Washington, D.C. 20350	1	Department of Physics & Chemistry Naval Postgraduate School Monterey, California 93940	1
Commander, Naval Air Systems Command Attn: Code 310C (H. Rosenwasser) Department of the Navy Washington, D.C. 20360	1	Scientific Advisor Commandant of the Marine Corps (Code RD-1) Washington, D.C. 20380	1
Defense Technical Information Center Building 5, Cameron Station Alexandria, Virginia 22314	12	Naval Ship Research and Development Center Attn: Dr. G. Bosmajian, Applied Chemistry Division Annapolis, Maryland 21401	1
Dr. Fred Saalfeld Chemistry Division, Code 6100 Naval Research Laboratory Washington, D.C. 20375	1	Naval Ocean Systems Center Attn: Dr. S. Yamamoto, Marine Sciences Division San Diego, California 91232	1
Mr. A. M. Anzalone Administrative Librarian PLASTE/C/ARRADCOM Bldg. 3401 Dover, New Jersey 07801	1	Mr. John Boyle Materials Branch Naval Ship Engineering Center Philadelphia, Pennsylvania 19112	1
		Dr. L. Jarvis Code 6100 Naval Research Laboratory Washington, D.C. 20375	1

DATE  
ILME  
—8